Enzyme and Microbial Technology 148 (2021) 109799

Contents lists available at ScienceDirect

Enzyme and Microbial Technology

journal homepage: www.elsevier.com/locate/enzmictec

Cloning, expression, biochemical characterization, and molecular docking studies of a novel glucose tolerant β-glucosidase from *Saccharomonospora* sp. NB11

Numan Saleh Zada [a,b], Ali Osman Belduz [b], Halil Ibrahim Güler [b], Anum Khan [a], Miray Sahinkaya [b], Arife Kaçıran [b], Hilal Ay [c], Malik Badshah [a], Aamer Ali Shah [a], Samiullah Khan [a,*]

[a] Department of Microbiology, Quaid-i-Azam University, Islamabad, 45320, Pakistan
[b] Department of Molecular Biology, Faculty of Sciences, Karadeniz Technical University, 61080, Trabzon, Turkey
[c] Department of Molecular Biology and Genetics, Faculty of Sciences and Arts, Ondokuz Mayis University, Samsun, Turkey

ARTICLE INFO

Keywords:
Novel β-glucosidase
Glucose tolerant
Saccharomonospora sp. NB11
Molecular docking

ABSTRACT

Most of the presently known β-glucosidases are sensitive to end-product inhibition by glucose, restricting their potential use in many industrial applications. Identification of novel glucose tolerant β-glucosidase can prove a pivotal solution to eliminate end-product inhibition and enhance the overall lignocellulosic saccharification process. In this study, a novel gene encoding β-glucosidase BglNB11 of 1405bp was identified in the genome of *Saccharomonospora* sp. NB11 and was successfully cloned and heterologously expressed in *E. coli* BL21 (DE3).The presence of conserved amino acids; NEPW and TENG indicated that BglNB11 belonged to GH1 β-glucosidases. The recombinant enzyme was purified using a Ni–NTA column, with the molecular mass of 51 kDa, using SDS-PAGE analysis. BglNB11 showed optimum activity at 40 °C and pH 7 and did not require any tested co-factors for activation. The kinetic values, K_m, V_{max}, k_{cat}, and k_{cat}/K_m of purified enzyme were 0.4037 mM, 5735.8 μmol/min/mg, 5042.16 s^{-1} and 12487.71 s^{-1} mM^{-1}, respectively. The enzyme was not inhibited by glucose to a concentration of 4 M but was slightly stimulated in the presence of glucose. Molecular docking of BglNB11 with glucose suggested that the relative binding position of glucose in the active site channel might be responsible for modulating end product tolerance and stimulation. β-glucosidase from BglNB11 is an excellent enzyme with high catalytic efficiency and enhanced glucose tolerance compared to many known glucose tolerant β-glucosidases. These unique properties of BglNB11 make it a prime candidate to be utilized in many biotechnological applications.

1. Introduction

Lignocellulosic materials comprise cellulose, hemicellulose, and lignin, in which cellulose and hemicellulose make up to two-third of lignocellulosic residues. These materials act as a potential renewable energy source such as biofuel production and account for a large part of agricultural and forestry wastes [1]. Producing biofuel from lignocellulosic biomass requires several steps: pretreatment, hydrolysis, fermentation, separation, and purification [2]. In these processes, enzymatic hydrolysis plays the most curial role as the efficient conversion of biomass to biofuels is limited by the adequate conversion of polymers to glucose [3].

The pretreated biomass is mainly hydrolyzed by a cellulolytic enzyme system yielding fermentable sugars as an end product [4]. A cellulolytic enzyme system predominantly consists of exocellulases (EC 3.2.1.91), endocellulases (EC 3.2.1.4), and β-glucosidases (Bgls) (EC 3.2.1.21). Bgls act upon cellobiose and other oligomers produced by exocellulases and endocellulases. Bgls act as a rate-limiting factor in the process. At a low concentration of β-glucosidase, cellobiose is accumulated, leading to feedback inhibition of the other two enzymes [5]. Therefore, it is crucial to overcome end-product inhibition to enhance the efficacy of cellulose hydrolysis.

To date, most of the known microbial Bgls are highly sensitive to glucose and their activity is predominantly reduced in the presence of

* Corresponding author.
E-mail address: samikhan@qau.edu.pk (S. Khan).

https://doi.org/10.1016/j.enzmictec.2021.109799
Received 24 December 2020; Received in revised form 10 March 2021; Accepted 2 April 2021
Available online 15 April 2021
0141-0229/© 2021 Elsevier Inc. All rights reserved.

glucose. The development of Bgls tolerant to glucose inhibition can have a considerable impact on cellulosic saccharification, accelerating the entire process of cellulose breakdown [6].

The problem of glucose inhibition is usually overcome by the addition of exogenous enzymes in the cellulolytic complex. Studies on improving the overall product yield by the addition of β-glucosidase are well documented [5]. Sadly, most of the commercially available cellulolytic complex for biomass hydrolysis lack Bgl [7]. Adding exogenous Bgl seems a promising solution, but its implementation is limited due to the cost of the enzyme. Therefore, bio-prospecting of a novel, cost-effective, and enhanced Bgl is under the spotlight these days.

The advances in molecular biology techniques such as molecular cloning have enabled researchers to produce enhanced yields of purified proteins and improve biotechnologically important enzymes by studying their structure/functional relationships. Production of Bgls from diverse microbial sources and studying their physicochemical properties are in practice over the last decade. These studies have allowed a comprehensive study of protein sequences, functions, families and catalytic domains.

Genus *Saccharomonospora* is gram-positive, aerobic, and catalase-positive bacteria belonging to the *Pseudonocardiaceae* family and are actinomycetes. These organisms form a coherent group in the actinomycete phylogenetic tree based on ribosomal RNA sequences [8].

In this study, high glucose tolerant Bgl has been identified and cloned from *Saccharomonospora* sp. NB11 genome. Multiple sequence alignment of BglNB11 to other GH1 Bgls shows that recombinant protein has characteristic conserved amino acid residues, NEPW and TENG at its active site, indicating that BglNB11 is a GH family1 protein. Molecular docking of BglNB11 with pNPG and glucose showed glucose binds to the middle of the active site channels in close proximity with pNPG. The binding of glucose to this position relative to the substrate can enhance substrate cleavage by transglycosylation, which can, in turn, stimulate enzyme activity [9]. Glucose molecule was also docked into glucose-intolerant Bgl *Trichoderma reesei* TrBgl2 and glucose tolerant MeBglD2 to determine glucose binding preferences. It is concluded in the current study that the position of glucose binding along the active site channel of the enzyme has a vital role in glucose modulation.

The term cold-active or cold-adaptive enzyme has been used extensively in the literature for the enzymes that are more stable at moderate temperatures [10–14]. Enzymes exhibiting stability at moderate temperatures are advantageous in many industrial applications because they can lower energy cost, protect thermosensitive substrates or end products, prevent unwanted chemical transformations and lower the loss of volatile compounds in the reaction [15]

In the current study, for the first time, Bgl from *Saccharomonospora* sp. NB11 was successfully cloned, expressed, purified and biochemically characterized. The recombinant protein showed high glucose tolerance and enhanced catalytic efficiency compared to other known glucose tolerance Bgls. These uniquely attributed properties of BglNB11 make it a prime candidate to be utilized in different bio-industrial applications. Studying novel Bgl and elucidating glucose tolerance and stimulation mechanisms can provide new insights into their structural/functional relationship through enzyme engineering.

2. Materials and methods

2.1. Substrate and chemicals

Para-Nitrophenyl β-D-glucopyranoside (pNPG), a synthetic substrate for Bgl, was procured from Sigma-Aldrich (St. Louis, MO, USA). Wizard Genomic DNA extraction kit, plasmid DNA isolation kit, Taq DNA polymerase, restriction enzymes, deoxynucleotide triphosphate, T4 DNA ligase was procured from Promega (Madison, WI, USA). TALON Metal Affinity Resin was purchased from Takara Bio Inc (Shiga, Japan). Reagent grade chemicals were obtained from Sigma-Aldrich and double distilled and deionized water was used to make solutions.

2.2. Bacterial strains, vectors, and media

Saccharomonospora sp. NB11 was generously provided for this study by the Department of Molecular Biology and Genetics, Ondokuz Mayıs University, Samsun, Turkey. pGEM-T Easy cloning vector (Promega A1360) and *Escherichia coli JM101* (NEB) host cells were used for cloning. A pET- 28a (+) vector (Novagen) and *Escherichia coli* BL21 (DE3) (NEB) host cells were used for the expression of recombinant protein. Luria Bertani (LB) medium supplemented with 50 μg/mL kanamycin or ampicillin was used for growing the *E. coli* host cells.

2.3. Gene cloning and sequencing of BglNB11

The gene encoding BglNB11 was amplified from the genomic DNA of *Saccharomonospora* sp. NB11. Following primers were used for amplification of full-length BglNB11 gene, BglNB11 *F* (5'- CCC ATg gAg gTT gTg gAA gCT g -3') as forward and BglNb11RHis (5'- CTC gAg TCA TTC TCg TCC TgC C -3') as a reverse primer, having *Nco1* and *Xho1* restriction sites (underlined) respectively. PCR conditions were performed as initial denaturation at 98 °C for 120 s, denaturation at 95 °C for 30 s, annealing 50 °C for 80 s, extension at 72 °C for 300 s, a total of 36 cycles.

Amplified PCR product was cloned into the *pGEM-T Easy* cloning vector system to generate pGEMBglNB11. The transformed colonies were confirmed by digesting the plasmids extracted from transformed cells and digesting them with the *EcoR1* restriction enzyme. Positive clones were confirmed by sequencing through Macrogen, Netherlands and similarities were analyzed by the GenBank Advanced Blast Program (NCBI, NIH, Washington DC).

Cloning of 1407 bp fragment into pET28a (+) was performed for the intracellular expression designated as pETBGLNB11. The expression was then achieved by transforming plasmids into *E. coli* BL21 (DE3) cells.

2.4. Overexpression of BglNB11 gene

The recombinant *E. coli* BL21 (DE3) cell harboring the pETBGLNB11 gene was grown to an optical density (OD_{600}) of approximately 0.6. Protein expression was induced with 0.5 mM isopropyl-D-thiogalactoside (IPTG) and growth was then maintained at 25 °C for another 16 h with shaking incubator at 150 rpm. Next, the harvesting of induced cells at 10,000 rpm for 6 min and resuspension in phosphate buffer (100 mM, pH 8.0) was performed. The intracellular proteins were then unconfined by sonicating the cells by Sartorius Labsonic M (80 % amplitude, 0.6 cycles for 5 min) on ice. Cell debris from the cell-free extract was removed by centrifugation at 14,800 rpm for 15 min.

The expressed enzyme from Bl21/ pETBGLNB11 was designated as BglNB11 having *a* theoretical calculated molecular weight of 51 kDa.

2.5. Purification of BglNB11

Purification of the expressed protein was achieved by Ni–NTA affinity-column chromatography using the manufacturer's guidelines. In this protocol, the wash buffer comprises 20 mM imidazole, 50 mM NaH_2PO_4 and 300 mM NaCl. The elution buffer contained 250 mM imidazole, while the concentrations of the salts remained the same.

2.6. Determination of protein concentration

The protein concentration was obtained by Bradford assay with bovine serum albumin as standard.

2.7. Determination of BglNB11 activity

The BglNB11 enzyme activity was routinely performed by spectrophotometer via pNPG as a substrate. The reaction mixture (250 μL) comprising 5 mM pNPG in phosphate buffer (pH 8), 125 μL of 50 mM phosphate buffer (pH 8) and 0.48 μg enzyme was incubated at 40 ℃ for

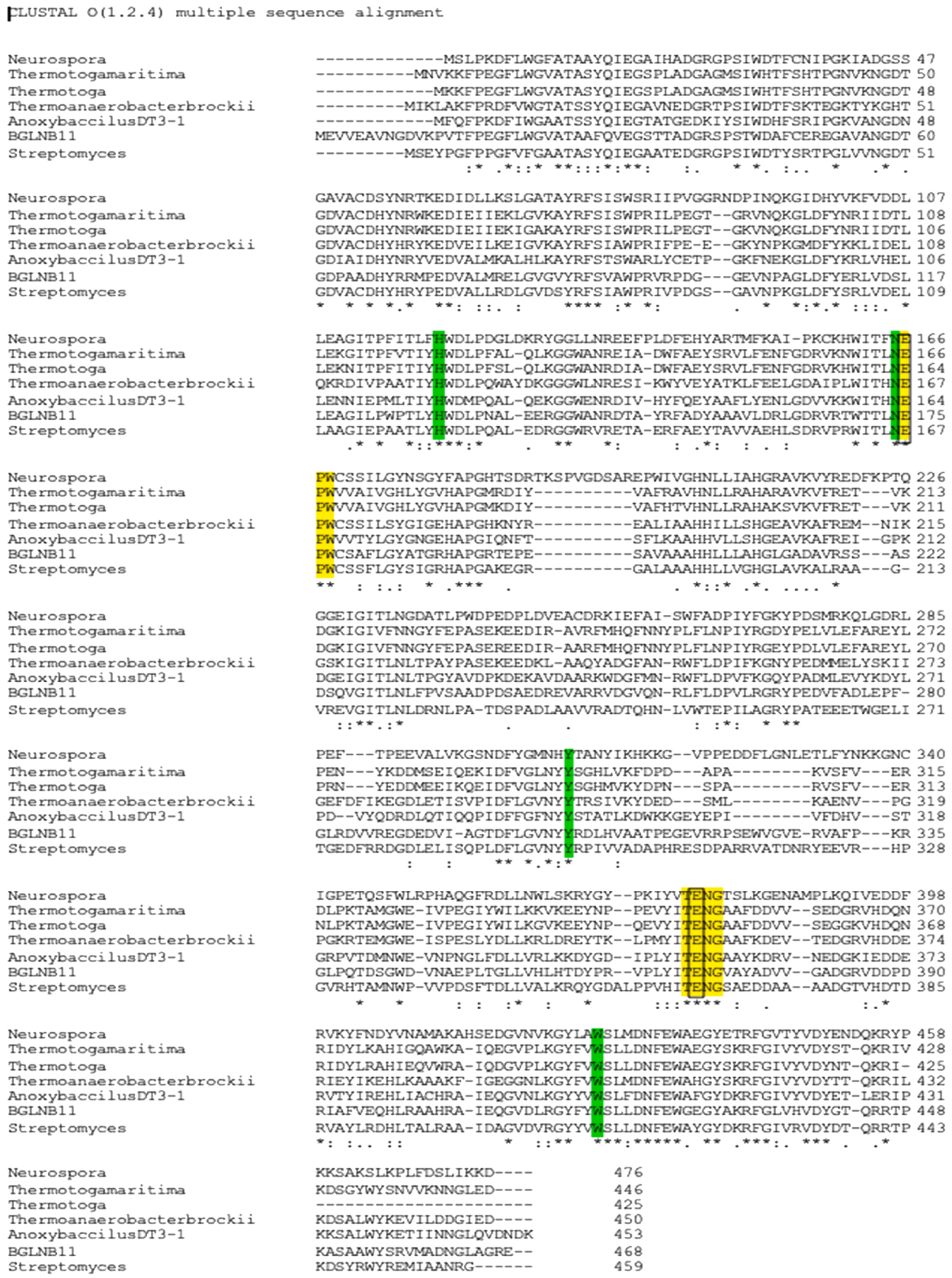

Fig. 1. Multiple sequence alignment of BglNB11 with other protein sequences from GH family 1 proteins. *Neurospora crassa* ID = U9W8B8), *Thermotoga maritima* (Uniport ID = Q08638), *Thermotoga neapolitana* (OX = 2337), *Thermoanaerobacter brockii* (Q60026) *Anoxybaccilus DT3-1* (Uniport ID = M5QUM2). *NB11* (This study), *Streptomyces coelicolor* (PDB ID = Q9K440). The catalytic nucleophile and acid/base residues are shown by the box; Yellow highlight indicates characteristic conserved catalytic motifs of GH1 β-glucosidases. The green highlight indicates putative conserved regions responsible for glucose tolerance in GH family 1 proteins.

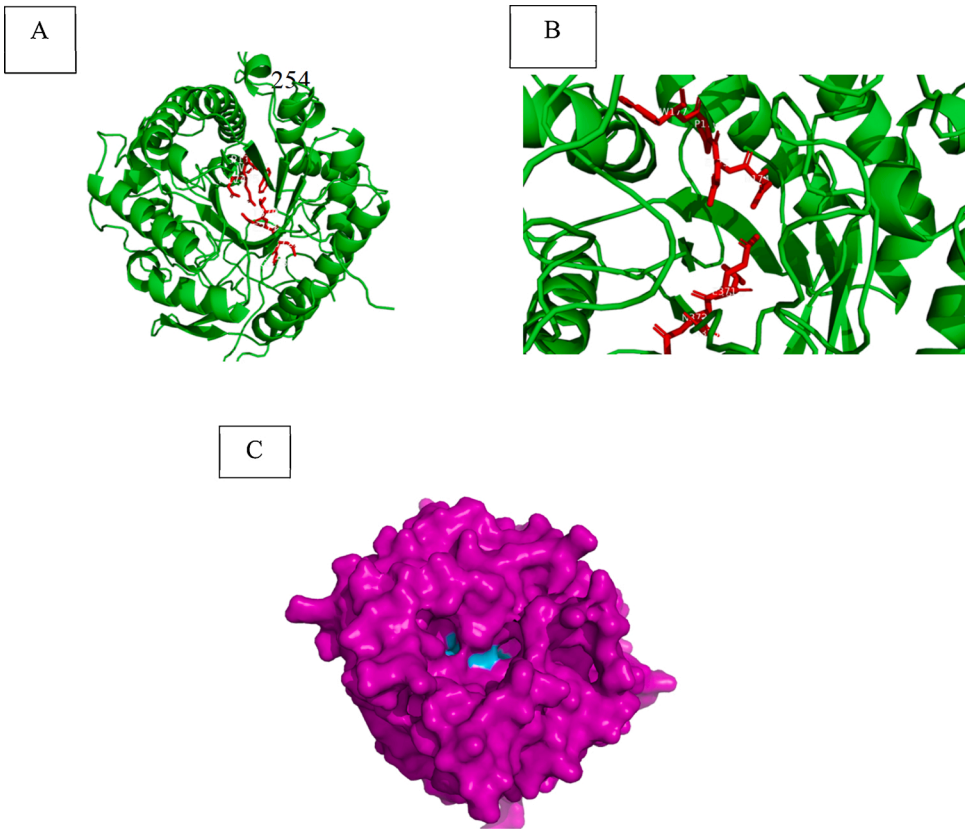

Fig. 2. A) Predicted 3D structure of BglNB11, B) GH1 conserved amino acid motifs are shown by red sticks, C). Surface representation of BglNB11, conserved catalytic residues are highlighted by cyan color.
*3D structure was predicted using homology modeling using SWISS-MODEL automated protein homology-modeling server (https://swissmodel.expasy.org/)
**Protein visualization was carried out using The PyMOL Molecular Graphics System, Version 1.8 Schrödinger, LLC.

30 min. The reaction was terminated by adding 750 μL of 1 M Na_2CO_3 and the color developed was measured at 405 nm by a spectrophotometer. A Blank without enzyme was used to substrate non-enzymatic components. The amount of enzyme needed to catalyze one μmol pNP/minute under defined assay conditions is referred to as one unit of enzyme activity.

2.8. Effects of temperature on activity and stability of BglNB11

The effect of temperature on BglNB11 activity was analyzed by spectrophotometer using pNPG as the substrate. The activity assays were performed over the temperature range of 25–70 °C under standard assay conditions and the results were expressed as relative activity (%). For the determination of temperature stability of BglNB11, the enzyme's incubation was performed over a temperature range of 25–60 °C, and its activity was performed after regular time intervals. The residual activity percentage of BglNB11 was measured by comparison with the untreated enzyme.

Table 1
β-glucosidases sharing high similarity with BglNB11.

S. No	Species	Sequence ID**	Identities (%)	Protein size (kDa)*
1	*Saccharomonospora azurea* NA-128	EHY87871.1	86	50.9
2	*Saccharomonospora glauca*	EIE99438.1	81	51.30
3	*Prauserella shujinwangii*	PRX45179.1	72	52.2
4	*Actinopolyspora iraqiensis*	WP_026452833.1	74	51.09
5	*Prauserella marina*	WP_091808970.1	72	51.42
6	*Amycolatopsis sp.* YIM 10	QFU89140.1	69	51.95
7	*Nocardia sp.* NRRL S-836	KOV83152.1	65	50.6

Note: The results were obtained by searching the BglNB11 protein sequence in the NCBI Blast database with default parameters.
* The protein sizes were predicted using the Expasy server ProtParam tool. (https://web.expasy.org/protparam/).
** The protein sequences for the comparison were retrieved from NCBI using their sequence IDs.

2.9. Effects of pH on activity and stability of BglNB11

The effects of pH on the activity of BglNB11 were determined at 40

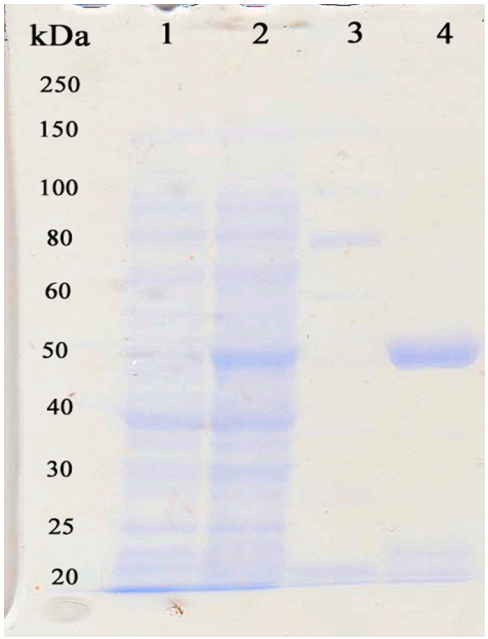

Fig. 3. SDS-PAGE analysis of BglNB11 Lane1: *E. coli Bl21 (DE3)* crude extract without BglNB11 gene. Lane 2: Crude extract of BglNB11, Lane 3: Molecular weight marker, Lane 4: The purified fraction of BglNB11 after Ni-NTA affinity chromatography column.

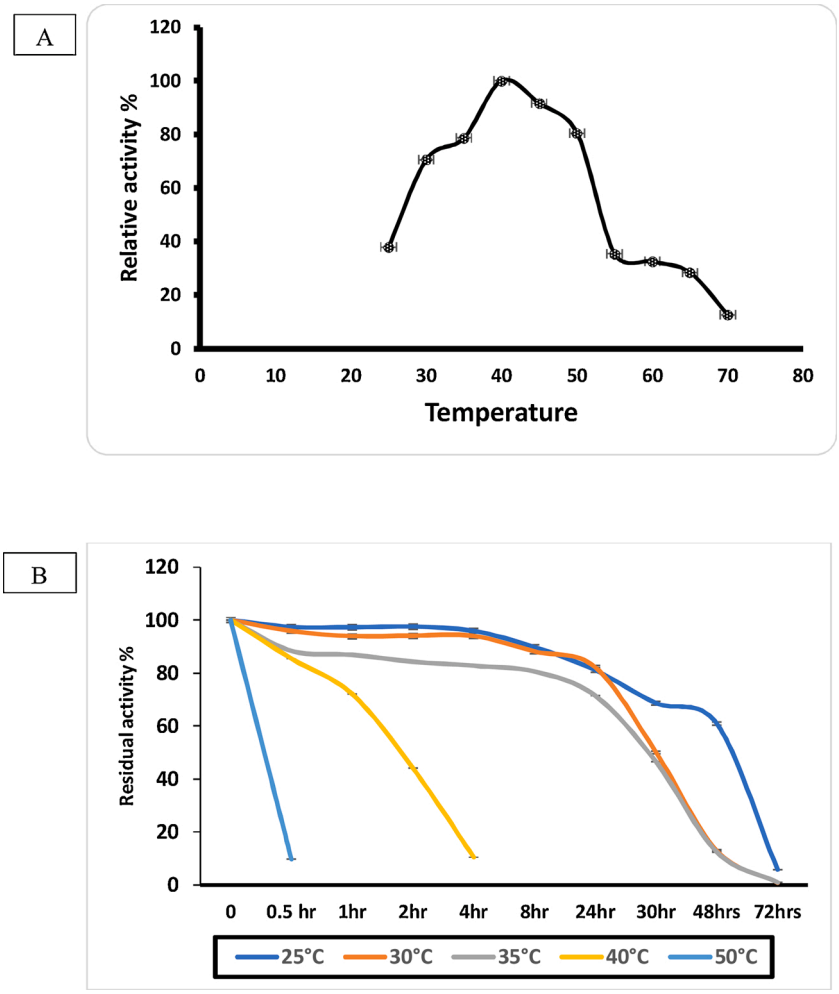

Fig. 4. (A). Effect of temperature on activity (A) and (B) stability of BglNB11. The effect of temperature on BglNB11 activity was analyzed in Phosphate buffer (pH 7). The activity determined at 40 °C was taken as 100 %. For determining the stability of BglNB11, the enzyme was pre-incubated at different temperatures (25 °C-50 °C) and enzyme activity was performed in regular intervals.

°C and 405 nm, spectrophotometrically under standard assay conditions. A 50 mM sodium citrate buffer (pH 3–5), and 50 mM sodium phosphate buffer (pH 6–7), 50 mM potassium phosphate buffer (pH 8), Glycine-NaOH buffer (pH 9–10) were used to determine the enzyme optimal pH.

The enzyme stability was checked using different pH values by pre-incubating the enzyme at different pH (3–10), and enzyme activity was taken after regular intervals as a function of residual activity as described above.

2.10. Effects of metal ions and reagents on BglNB11 activity

The effects of metals ions were determined using $NiCl_2$, $MgCl_2$, $FeSO_4$, $CaCl_2$, $MnSO_4$, $CoCl_2$ $ZnCl_2$, KCl, $HgCl_2$, $CuSO_4$ and NaCl salts. Enzyme was pre-incubated with 0.5 mM, 1 mM and 2 mM metal salts at 40 °C for 30 min. The effect of reagents; Triton X-100, SDS, Tween 20 (1% v/v, 5% v/v and 10 % v/v), organic solvents Dioxane, DMSO, propanol, ethanol, methanol, butanol (5%, 10 % v/v and 20 % v/v), and other chemicals DTT, DEPC, EDTA, EGTA and PMSF (1 mM, 5 mM, 10 mM) were determined by incubating reagent at 40 °C for 30 min and enzyme action was then performed under standard assay conditions.

BglNB11 activity without metal salts and reagents was referred to as 100 % for determining the residual activities (%).

2.11. Effect of glucose on BglNB11 activity

The glucose effect on the activity of purified BglNB11 was estimated using pNPG as substrate at different concentrations of glucose ranging from 200−4000 mM under standard assay conditions. Pre-incubated enzyme without glucose addition was taken as control and represented as 100 % for calculating relative activities.

2.12. Enzyme kinetics

Michaelis-Menten constant (Km), maximum velocity (Vmax) of BglNB11 were determined by measuring the hydrolysis rate of pNPG at various concentrations (0.2−6 mM) at 40 °C for 30 min in 50 mM phosphate buffer (pH 8). Michaelis-Menten plotting was performed using the obtained data.

2.13. Protein-ligand interactions through molecular docking

To understand the interactions of BglNB11 with pNPG and glucose, a model BglNB11 protein structure was generated by a SWISS-MODEL automated protein homology-modeling server with the Bgl from Metagenomic glucose-tolerant glycosidase (PDB ID: 5XGZ) [16] as a template. Bgl from *Trichoderma reesei* (TrBgl2) (PDB ID = 3AHY), [17] was used for comparison as glucose intolerant Bgl and Metagenomic glucose-tolerant glycosidase MeBglD2 (PDB ID = 5XGZ) was used for

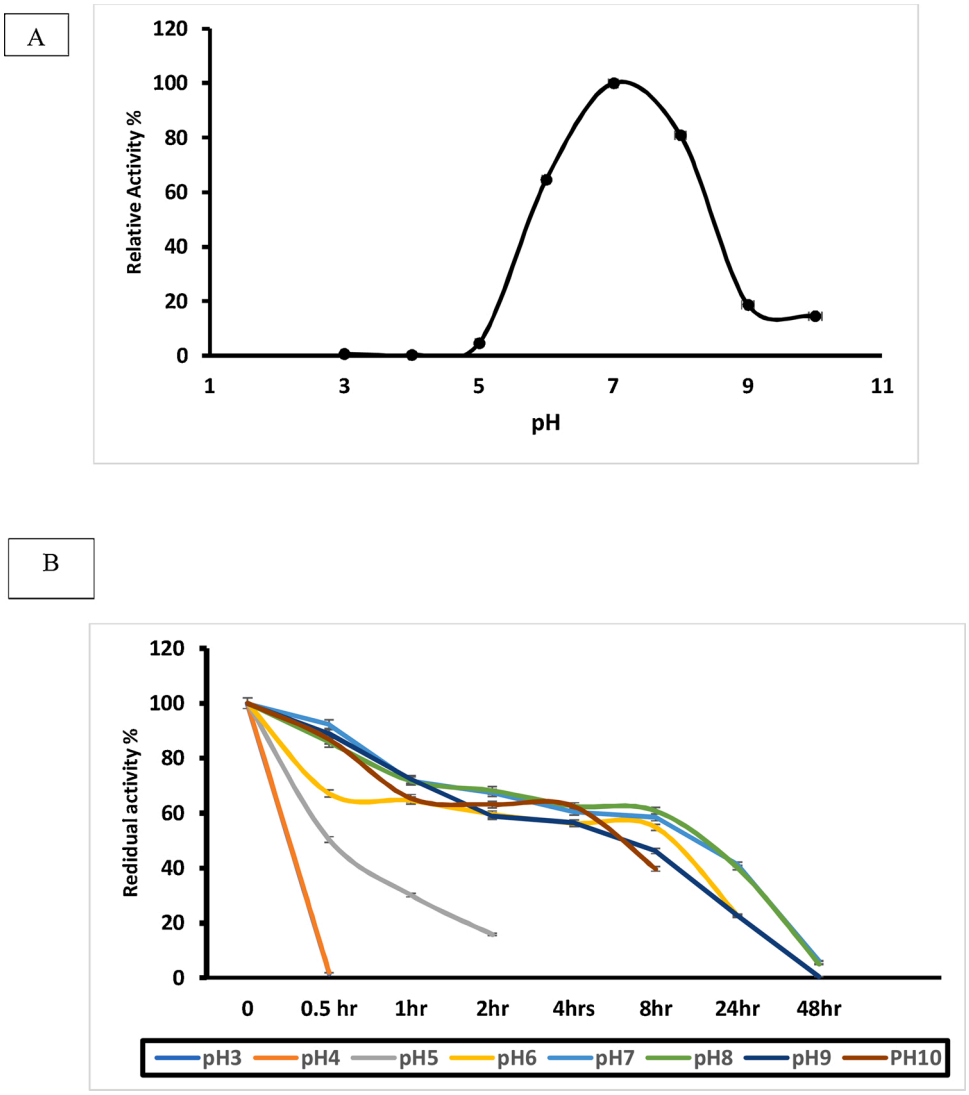

Fig. 5. Effect of pH: (A). activity and (B) stability of BglNB11. The effect of pH on BglNB11 activity was analyzed at 40 °C. The activity determined at pH 7 was taken as 100 %. For determining the stability of BglNB11 at different pH, the enzyme was pre-incubated at different pH ranges (pH 3-pH 10) and enzyme activity was performed after regular intervals.

comparison as glucose tolerant Bgl. The protein model was analyzed using PyMol molecular visualizing software. The data on pNPG and glucose's chemical structures were downloaded in SDF file format from PubChem database (https://pubchem.ncbi.nlm.nih.gov/) and converted to PDB file format using BIOVIA Discovery Studio Visualizer 2018 (Dassault Systèmes BIOVIA, 2016). Potential pNPG and glucose binding sites in the substrate channel were discovered by using AutoDock 4.0. Essential polar hydrogen atoms and Gasteiger charges were employed using AutoDock tools. The ligand was also prepared using AutoDock tools; torsion angles were assigned to ligand and docking was carried out AutoDock Lamarckian Genetic Algorithm (LGA, runs 100). Protein molecule (receptor) was enclosed in a grid and ligands were subjected to move within the enclosed grid to attain the lowest energy conformation. Results were generated with AutoDock and the lowest energy conformation was employed for further analysis.

3. Results and discussion

3.1. Protein sequence analysis

The gene (1407 bp) was amplified from the genome of *Saccharomonospora* sp. NB11. (GenBank accession number: JACBJG000000000). The calculated molecular weight of the protein was around 51 kDa. Multiple sequence alignment of BglNB11 with GH1 Bgls from other species revealed that the sequence contains highly conserved sequences in its active site. BglNB11 possesses the characteristic NEPW (amino acid 174–177) and TENG (370–374) conserved active-site motifs of the GH1 Bgl (Fig. 1). The residues Glu175 and Glu371 act as the catalytic acid-base and nucleophile, respectively (Fig. 2).

The BglNB11 predictable 3D structure shows a typical (β/α) 8-barrel structure observed in other structurally characterized GH1 (Fig. 1). A BglNB11 showed 65–86 % similarity to homologous Bgls available in genomes of neighboring taxa (Table 1). To date, no similar proteins have been biochemically characterized.

3.2. Expression and purification of BglNB11

After expression, the recombinant protein was obtained as soluble fractions in large quantities. On the contrary, Bgls from some other microorganisms such as *Thermotoga neapolitana* [18] and *Thermotoga thermarum* [19] formed the insertion body in *E. coli* host cells.

Ni-NTA column eluted fractions of purified BglNB11 were pooled together and analyzed by SDS PAGE. A single band corresponding of

around 51 kDa was observed (Fig. 3). The observed molecular weight supported the theoretical calculated molecular weight of BglNB11.

3.3. Effects of temperature and pH on activity and stability

The effect of temperature on activity and stability of BglNB11 was studied over a temperature range of 25−70 °C and pH 3−10. The enzyme exhibits maximum relative activity at 40 °C, while its relative activity was more than 70 % at the temperature range from 35 °C to 50 °C [Fig. 4(A)]. A drastic decline in enzyme activity was observed above 50 °C. The optimum activity of BglNB11 was comparable with other Bgls, which have optimum activity at mild temperatures. BglNB11 has a similar optimum temperature of 40 °C as *Alteromonas* sp. L82 [10] and *Bacillus cellulosilyticus* [11] Bgls, while higher than *Serratia* sp. TN49, which has optimum activity at 35 °C [20]. BglNB11 retained 40 % of its original activity after pre-incubation at 40 °C for 2 h while retaining more than 70 % of its residual activity after 24 h at temperature 25−35 °C. (Fig. 4B). BglNB11 exhibits the behavior of typical cold-active enzymes showing denaturing by heat at a temperature above 50 °C [21].

Notably, the thermal stability profile of BglNB11 at 40 °C was found higher than other cold-active enzymes such as Bgl from *Alteromonas* sp. L82; having a half-life of 20 min at 40 °C [10] and *Serratia* sp. TN49 showing a half-life of 1 h around 40 °C [20]. Cold-adapted enzymes have particular advantages in the food industry, helping maintain original food flavor and reducing overall energy consumption needed for the enzymatic process [22].

The optimum pH of BglNB11 was studied over a pH range of 3–10 at temperature 40 °C. The enzyme showed maximum activity at pH 7, while its relative activity was more than 60 % at pH 6 and 8. BglNB11 activity was lost rapidly at pH below 6 and above 8 [Fig. 5(A)]. Additionally, the enzyme retained more than 50 % residual activity after 8 h pre-incubation at pH 6−10. After 24 h of pre-incubation at pH 7, the enzyme retained 41 % residual activity indicating that it is stable at neutral pH. An apparent decline in enzyme activity was observed when pre-incubated at pH below 6 [Fig. 5(B)]. Thus, BglNB11 is active and stable at pH around 6−8. This result is comparable to most of the Bgls, such as *Bacillus cellulosilyticus, Serratia* sp. TN49, marine microbial metagenome and *Paenibacillus xylanilyticus*KJ-03 [11,20,23–25]. These pH stability properties of BglNB11 are desirable attributes for industries such as food and wine and lignocellulose utilizing biorefineries.

3.4. Effect of metals on the activity of BglNB11

The influence of different metal salts (0.5 mM–2 mM) on BglNB11 activity was investigated (Fig. 6). $ZnSO_4$, $CuSO_4$, and $HgCl_2$ had a strong inhibitory effect on the activity of BglNB11. Comparable results were also observed from Bgls from *Paenibacillus xylanilyticus*KJ-03 [24], *Anoxybacillus* sp. DT3-1 [25], *Martelella mediterranea* [13]. The heavy metals inactivate enzymes by reacting with the sulfhydryl group of cysteine bonds, where they form a covalent bond with the sulfur atom and hydrogen ion are replaced [26]. Similarly, $CoCl_2$ and $MnSO_4$ also had an inhibitory effect on enzyme activity on higher concentrations (2 mM); these results are consistent with the studies conducted on *Alteromonas* sp. L82 [10] and *Jeotgalibacillus malaysiensis* [27]. Enzyme activity was not affected in the presence of 0.5 mM $NiCl_2$, $MgCl_2$, $FeSO_4$, $CaCl_2$, and KCl, but some inhibitory effects were observed at higher concentrations (1 mM and 2 mM). From the reported studies, $CaCl_2$ has an inducing effect on Bgls activity from *Weissella cibaria, Reticulitermes flavipes, Exiguobacterium* sp. DAU5 [28–30]. $MgCl_2$ and KCl also increased activities of β-glucosidase from *Jeotgalibacillus malaysiensis* [27], *Cellulomonasmicrobium cellulans* [31], and *T. thermosaccharolyticum* [32]. Contradictory results were observed for BglNB11 for the above metals. In most of the reports, Bgl activity was inhibited by $NiCl_2$ and $FeSO_4$ [27,33]; contrary results were observed for BglNB11. These findings suggest the need further to explore interactions of metal ions at active site pockets to help unveil reasons for metal dependencies of Bgls. BglNB11 is active in the presence of most of the tested metal ions, which indicates its potential as an industrial enzyme.

3.5. Effect of chemicals and other reagents on the activity of BglNB11

Among the tested detergents, SDS showed a high inhibitory effect on the activity of BglNB11 (Fig. 7A). Triton X-100 and Tween 20 retained more than 85 % residual activity up to 10 % v/v concentration. Strong inhibition by SDS can be attributed to the fact that the SDS reacts with the enzyme's hydrophobic regions causing the unfolding of native enzyme structure resulting in enzyme denaturation [34].

The BglNB11 activity was not affected by tested organic solvents at concentration 5% v/v except butanol which had a strong inhibitory effect (Fig. 7B). At higher concentrations, organic solvents had an inhibitory effect on BglNB11 activity. Enzyme retained more than 60 % of its residual activity in the presence of 20 % v/v methanol. Studies of

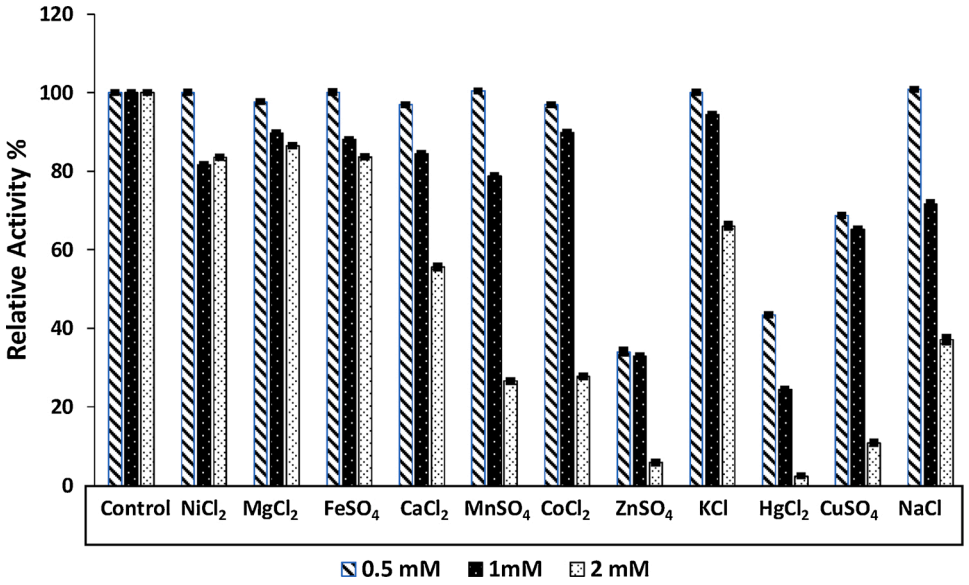

Fig. 6. Effect of different metal salts on BglNB11 activity. Enzyme activity lacking metal was taken as control. The enzyme was pre-incubated at 40 °C with varying concentrations of metal salts and enzyme activities were performed after a fixed interval.

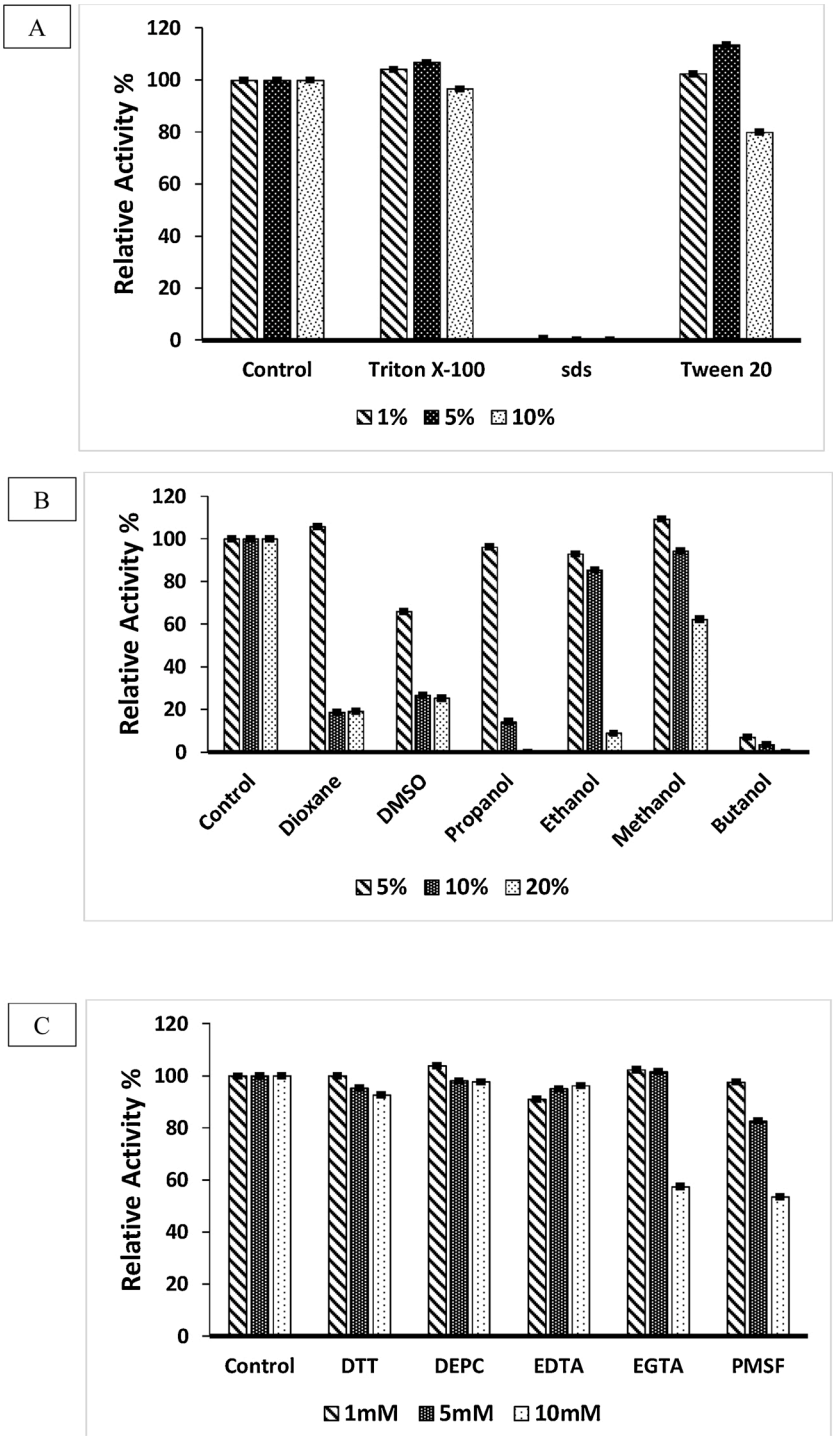

Fig. 7. Effect of (A) Detergents and (B) organic solvents, and (C) other chemicals on BglNB11 activity. BglNB11 was pre-incubated with detergents, organic solvents and other chemicals at 40 °C for 30 min, after which enzyme assay was performed under standard assay conditions. The activity of enzymes without metals or chemicals was taken as control and refereed as 100 % for relative activity determination.

β-glucosidases from other microorganisms showed a similar effect to organic solvents [10,27,35].

The effect of different chemicals, DTT, DEPC, EDTA, EGTA and PMSF, on the activity of BglNB11 is shown in (Fig. 7C). EDTA did not inhibit enzyme activity, indicating that BglNB11 is not a metalloenzyme. BglNB11 retained its activity against most of the tested chemicals.

BglNB11 ability to work in the presence of most chemicals and reagents can find its way in textile, paper and pulp and many other industries.

3.6. *Effect of glucose on BglNB11 activity*

BglNB11 activity was not affected by a considerably higher concentration of glucose (4 M). BglNB11 showed higher glucose tolerance than most of the currently known Bgls (Table 2). Another important characteristic of BglNB11 is that its activity is slightly stimulated in the presence of glucose (Fig. 8). A similar effect was also observed by Bgls from *Anoxybacillus* sp. DT3-1 [25], *bgl1A* from Marine Microbial Metagenome [10], *Scytalidium thermophilum* [36], and *Streptomyces* sp. [37].

Table 2
Comparison of characteristics of glucose tolerant β-glucosidases from different organisms using pNPG as substrate.

Organism	Optimum pH	Temperature (°C)	Glucose tolerance (mM)	Km (mM)	Vmax (μmol/ min/ mg)	K_{cat} (s^{-1})	K_{cat} /K_m (mM^{-1} s^{-1})	Reference
Saccharomonospora sp. NB11	7	40	4000	0.4037	5735.8	5042.16	12487.71	This study
Bacillus cellulosilyticus	7	40	200	2.97	66.2	70.3	ND*	[11]
Alteromonas sp. L82	7	40	700	0.55	83.6	74.3	135.1	[10]
Marine Microbial Metagenome	6.5	40	1000	0.39	50.7	ND*	ND*	[23]
Candida peltata	5	50	1400	2.3	108	ND*	ND*	[39]
Aspergillus oryzae	5	50	1300	0.55	1066	ND*	ND*	[40]
Debaryomyces vanrijiae	5	40	439	1.07	47.6	140.7	2.43	[41]
Termite gut	8	50	2250	0.134	ND*	163.2	1217.9	[42]

* ND = Not determined.

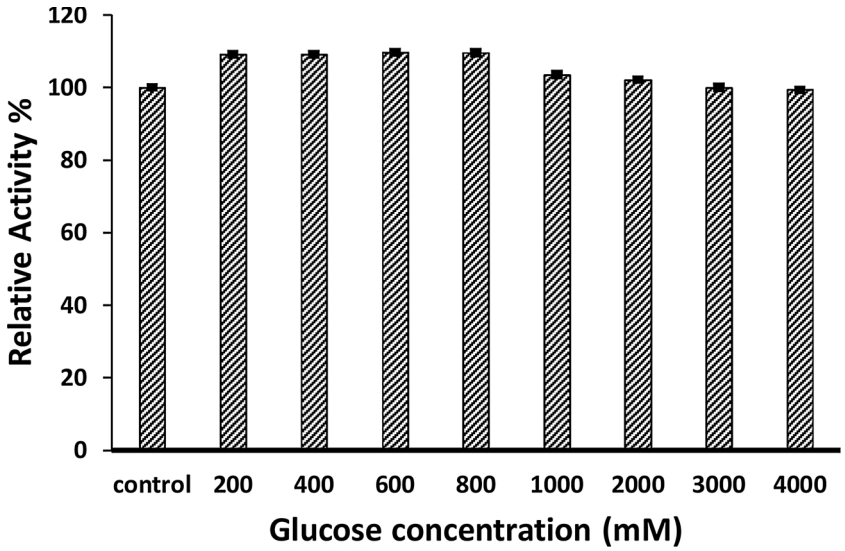

Fig. 8. Effect of glucose on the activity of BglNB11. The enzyme was pre-incubated with glucose at various concentrations (200 mM-4 mM) for 30 min, after which enzyme activity was performed under standard assay conditions. Enzyme activity without glucose addition was taken as control 100 % and residual activities are calculated relative to control.

This enzyme property can be exploited in industrial procedures such as enzymatic hydrolysis of lignocellulosic materials since most of the Bgls are inhibited by the end product glucose.

Some studies have gone underway to determine amino acid residues responsible for glucose tolerance. One particular study by Mariano et al. [38] have used bioinformatics analysis, such as docking and multiple sequence alignments, and found six residues conserved in all glucose tolerant Bgls. The conversed residues are H130, N174, E175, Y305, E371, and W418 (numbering corresponds to BglNB11) Fig. 1. These conserved residues in BglNB11 and other glucose tolerant Bgls indicate that these residues might have an essential role in glucose tolerance characteristics. However, the molecular basis of glucose tolerance due to these residues are not yet fully enlightened. Nonetheless, detailed insight into structural aspects of interactions with substrates and conserved residues is needed. In this study, we performed homology modeling with Bgls having varying glucose tolerance profiles to explain possible reasons for glucose modulations

3.7. Kinetic parameters

BglNB11 kinetic parameters were measured spectrophotometrically by Michaelis–Menten plots with pNPG using as substrate. The enzyme was incubated with different concentrations of pNPG ranging from 0.2−5 mM at 40 °C for 30 min in 50 mM phosphate buffer (pH 8).

BglNB11 exhibited K_m, V_{max}, k_{cat}, and K_{cat}/K_m values of 0.4037 mM, 5735.8 μmol/min/mg, 5042.16 S^{-1} and 12487.71 S^{-1} mM^{-1} respectively. The kinetic efficiency and glucose tolerance of BglNB11 are higher than most of the known glucose tolerant Bgls. The detailed comparison of kinetic parameter values and glucose tolerance of Bgls from different sources using pNPG as substrate are presented in Table 2.

3.8. Homology modeling and molecular docking

The BglNB11 3D structure was modeled by using SWISS-Model homology modular system with the crystal structure of Metagenomic glucose-tolerant glycosidase (PDB ID: 5XGZ) used as the template. Fig. 9 shows docked complex of BglNB11 with PNPG. This complex involved residues Gln30, Cys178, Arg188, and Trp426; these residues interact via hydrogen bonds with ligand and play an essential part in enzyme-substrate hydrolysis.

This interacting system was surrounded by His130, Trp131, Glu175, Trp177, Leu182, Asn231, Phe233, Tyr305, Val327, Glu328, Glu371, Arg306, Trp418 and Glu425 taking part in imparting hydrophobicity to the enzyme-substrate system. The two conserved GH1 residues Glu175 and Glu371, act as catalytic acid/base and nucleophile. These residues are highly conserved among GH1 Bgls and are considered essential for enzyme functions (Fig. 2). A detailed discussion about the importance of these residues is discussed elsewhere. [43]

In an effect to demonstrate the possible mechanism of glucose modulation on Bgls activities through molecular docking, a glucose-stimulated Bgl (BglNB11 in this study), glucose-intolerant Bgl *Trichoderma reesei* (TrBgl2) (PDB ID = 3AHY) [17] and glucose tolerant Bgl

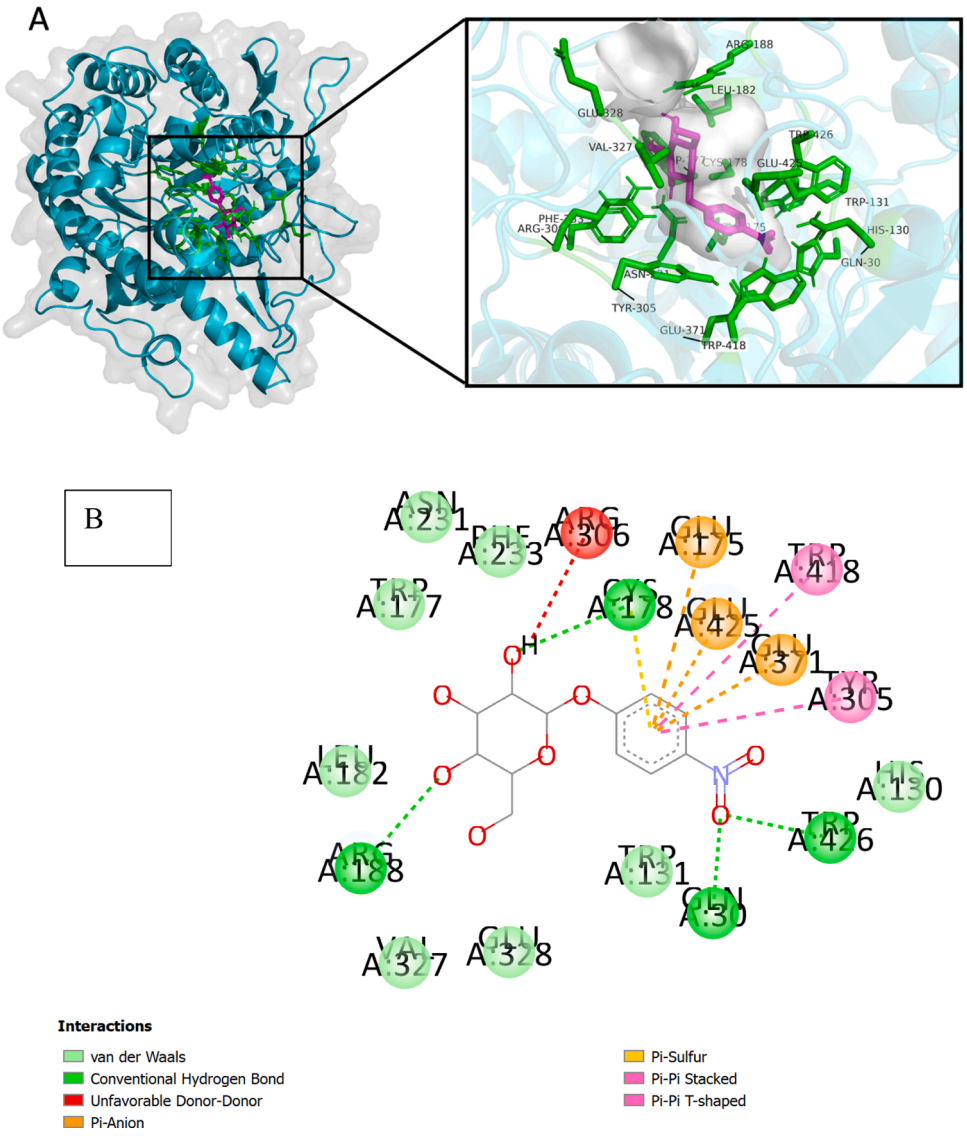

Fig. 9. Interaction analysis of BglNB11 with the substrate (pNPG). A) Cartoon representation of BglNB11: pNPG docked in BglNB11 shown in magenta color and represented as sticks. The interacting residues are shown in green color and represented as sticks. B) Two-dimensional (2D) view of pNPG interactions with BglNB11. The images were created using PyMOL (http://www.pymol.org) and Discovery studio visualizer (discover.3 ds.com).

MeBglD2 (PDB ID = 5XGZ) [16] were chosen. The molecular docking of Bgls with different glucose modulations emphasizes the binding of glucose along active site channel with varying preferences. The response of Bgl depends on the relative preference of glucose binding to different sites. The enzyme activity is inhibited when glucose is bound to the bottom of the active site channel. It makes several contacts with substrate binding residues leading to competitive inhibition of real substrate. Bgl is tolerant to end-product inhibition when glucose is bound to the site other than the active site, not interacting with active site residues. Stimulation of activity in the presence of glucose may result from the position of certain binding sites, where the bound glucose will enhance substrate cleavage activity through transglycosylation or other mechanisms such as allosteric effects.

Docking of glucose in TrBgl2 (glucose intolerant Bgl) indicated glucose preferred binding location at the button of the active site pocket, whereby making several contacts via hydrogen bonding with active site residues such as Cys 168, Glu 165, Trp 120, Trp 425, Glu 367, Trp 417, Glu 424 (Fig. 10). The interaction of glucose with these residues might result in competitive inhibition in the presence of real substrates such as pNPG. Thus, supporting the idea of inhibition of enzyme activity of TrBgl2 in the presence of glucose.

The docking analysis of glucose tolerant Bgl MeBglD2 showed no significant interaction of glucose with active site residues. The preferred binding location of glucose is other than the substrate binding position. Glucose molecule interacts with residues Asp 328 and Val 318 via hydrogen binding where it is not involved in competitive binding with substrates (Fig. 11). Consequently, MeBglD2 activity is not inhibited in the presence of glucose.

The docking of BglNB11, which is stimulated in the presence of glucose, revealed binding of glucose in the middle of the active site channel located closely to the substrate-binding site, making several contacts, some of which are overlapping (Fig. 12). Some of the overlapping binding sites include Trp 426, Glu 425, Typ 355, Glu 371. Yang et al. demonstrated that the relative position of glucose and substrate in the middle of the active site channel can excite the substrate's cleavage by transglycosylation, employing an allostatic effect. Our docked configuration results are in consensus and extend the observations made by Yang et al. [44].

These observations can be a step forward in understanding glucose dependence on activities of Bgl. Additionally, a recent study by Priscila et al. [45] emphasized that the narrow and deep active site channel of glucose tolerant Bgl restricts access glucose to the channel's active site

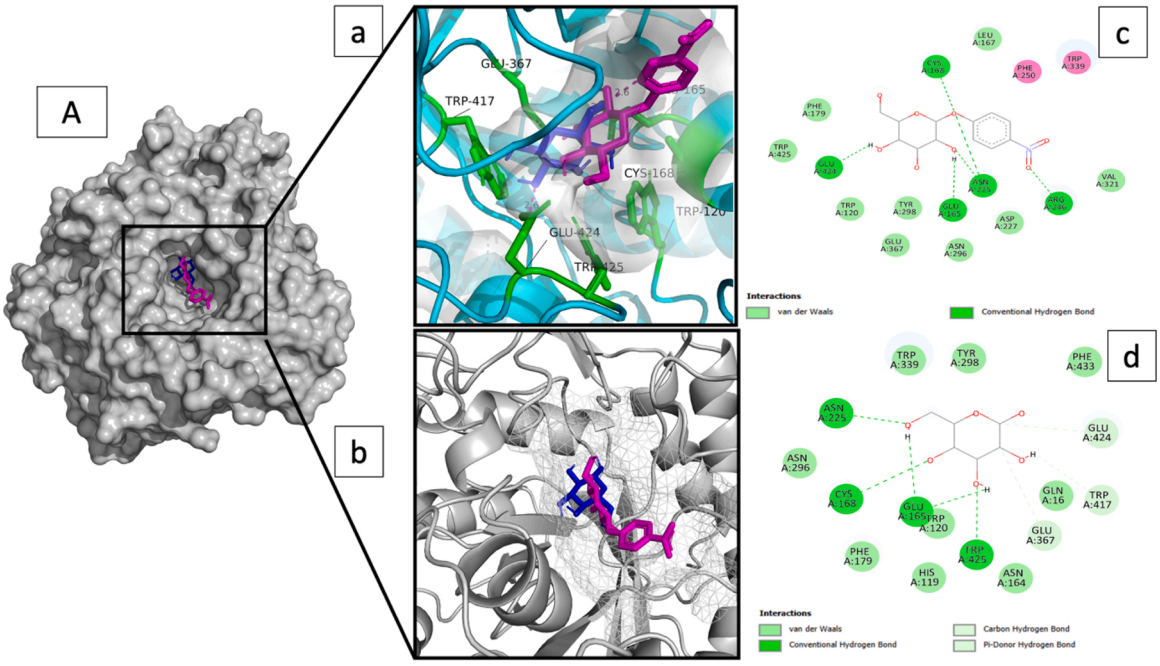

Fig. 10. Docking of glucose and pNPG in TrBgl2. **(A):** surface representation of TrBgl2 demonstrating the binding position of glucose and pNPG in active site pocket; glucose molecule shown in blue and pNPG magenta color. **(a):** Position and interaction of glucose with active site residues. The interacting residues Cys 168, Glu 165, Trp 120, Trp 425, Glu 367, Trp 417 and Glu 424 are shown in green color and presented as sticks. **(b)**: Mesh representation of active site pocket; the figure shows binding of glucose in the bottom of active site channel. **(c)**: Two-dimensional (2D) representation of interacting residues with pNPG and **(d)**: 2D representation of residues interacting with glucose. The images were created using PyMOL (http://www.pymol.org) and discovery studio visualizer (https://www.3ds.com/biovia).

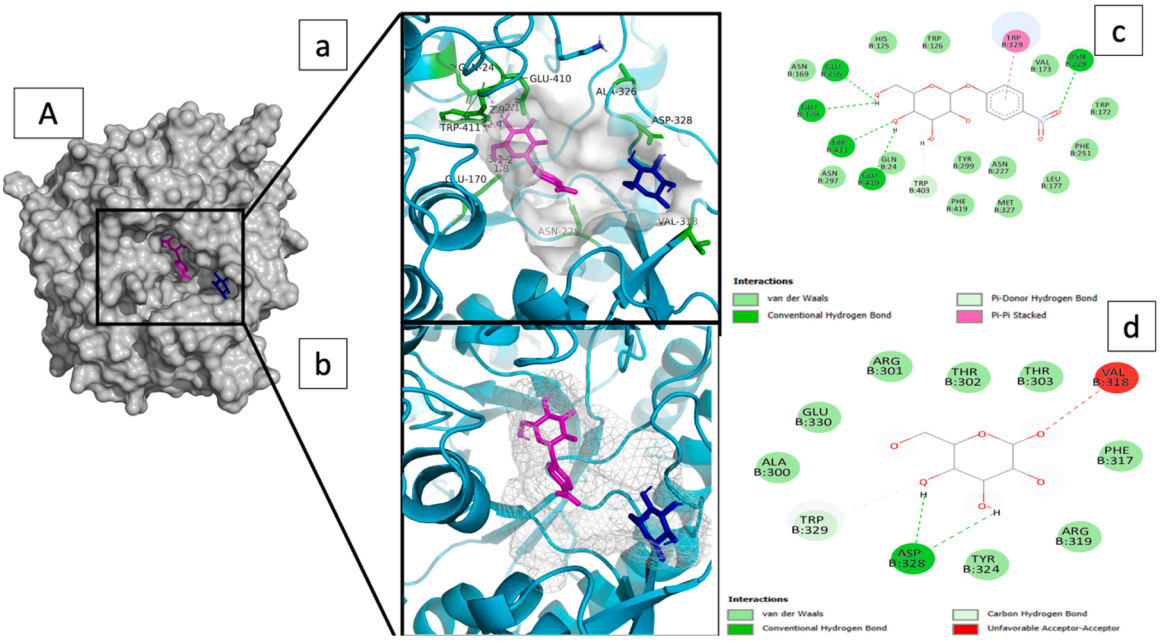

Fig. 11. Docking of glucose and pNPG in MeBglD2: **(A)** Surface representation of MeBglD2 demonstrating the binding position of glucose and pNPG in active site pocket; glucose is shown with blue color and presented as sticks and pNPG magenta color and presented as sticks**. (a)**: Position and interaction of glucose with residues Asp 328 and Val 318 via hydrogen bonding. **(b):** Mesh representation of active site pocket; Glucose is bound at a site other than active site residues. **(c)**:2D representation of interacting residues with pNPG and **(d)**: 2D representation of residues interacting with glucose. The images were created using PyMOL (http://www. pymol.org) and discovery studio visualizer (https://www.3ds.com/biovia).

and transglycosylation facilitated; therefore, competitive inhibition is avoided, which results in glucose tolerance and stimulation. However, Priscila et al. study did not explain why substrates containing glucose molecules were not omitted by narrow and deep active site channel. Additionally, the study did not take into account GH1 Bgls intolerant to glucose. Therefore, whether this mechanism applies to all Bgls remains doubtful. By comparing the active site of TrBgl2and MeBglD2, it was observed that TrBgl2 has a smaller active site pocket volume than MeBglD2. The observation about active site modulations due to the active site pocket's geometry was contradicted in our studies.

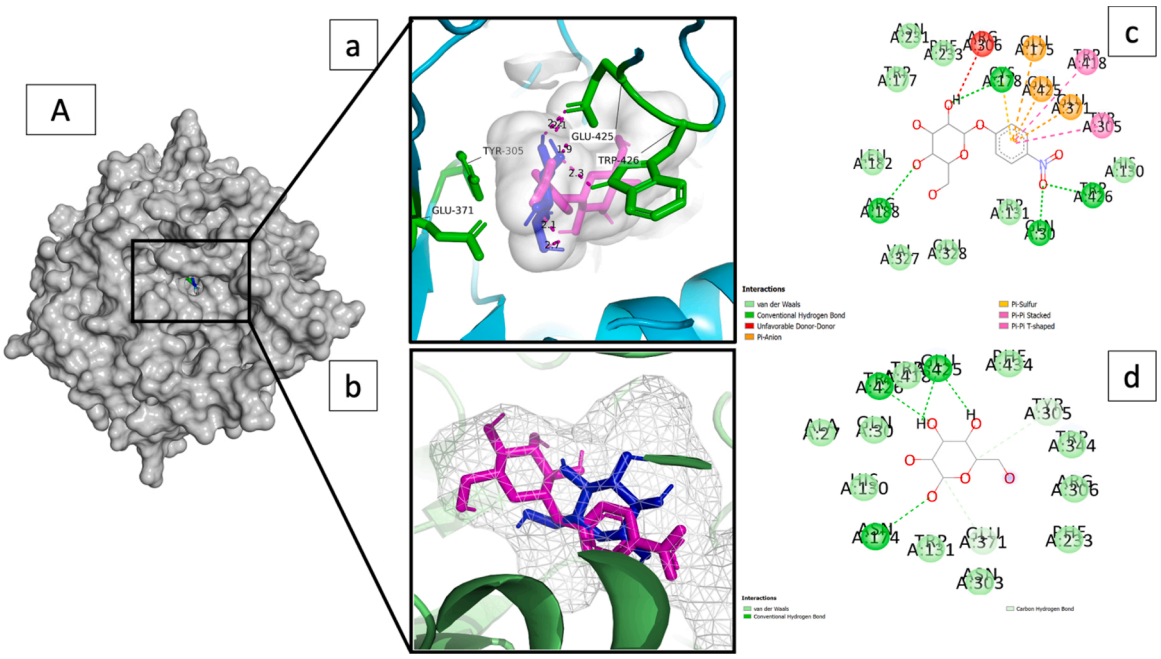

Fig. 12. Docking of glucose and pNPG in BglNB11. (A): Surface representation of glucose and pNPG docked in BglNB11. **(a):** Binding of glucose and pNPG in active site channel. Glucose is present in blue color and presented as sticks and pNPG in magenta color and presented as sticks. The overlaying interacting residues include Trp 426, Glu 425, Typ 355, Glu 371, are shown in green color and presented as sticks. **(b)**: Mesh representation of active site pocked showing relative binding positions of pNPG and glucose. **c)**: Two-dimensional (2D) representation of interacting residues with pNPG and **(d)**: Two-dimensional (2D) representation of residues interacting with glucose. The images were created using PyMOL (http://www.pymol.org) and discovery studio visualizer (https://www.3ds.com/biovia).

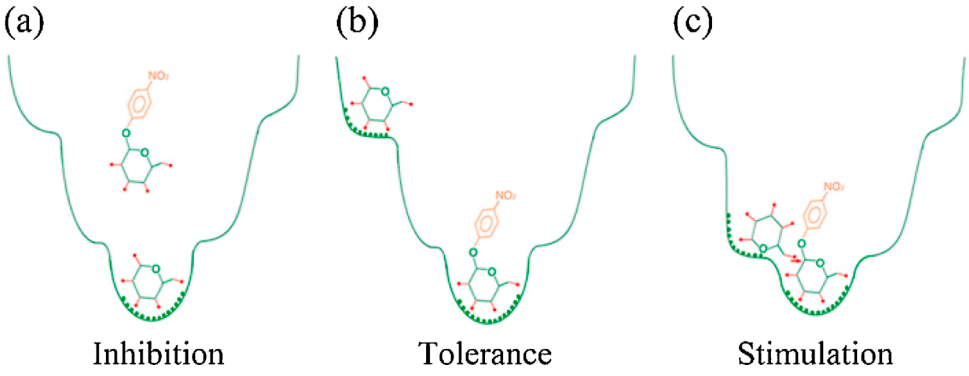

Fig. 13. Illustrative representation of glucose preferred binding site and its effect on the activity of Bgl. (a) Binding of glucose to the bottom of the active site leading to end-product inhibition. (b) The binding of glucose to the outside of the active site channel enables the enzyme to be glucose tolerant. (c) Binding of glucose at the middle of the active site results in the stimulation of enzymes in the presence of glucose. (Figure adapted from Yang et al. [44]).

(supplementary Fig.). Thus, there must be other factors than accessibility due to the active site pocket geometry, which contribute to glucose modulations in Bgls. Nevertheless, our molecular docking observations can provide a substantial baseline in understanding glucose dependencies on Bgl activity (Fig. 13).

4. Conclusion

In this study, novel glucose tolerant and cold-active β-glucosidase BglNB11 from *Saccharomonospora* sp. NB11 was cloned and biochemically characterized for the first time. BglNB11 was active at neutral and slightly alkaline conditions with stability at moderate temperatures. The enzyme has enhanced catalytic efficiency than most of the glucose tolerant Bgls. Our molecular docking study suggested binding position of glucose along the active site channel can contribute to overall glucose dependence in Bgls. The mechanism may be extended to other Bgls and can provide a start point for molecular development of Bgls, intolerant to end-product inhibition for better industrial utilization.

Authors contribution

NSZ: Took part in cloning, expression, purification, and molecular docking. Took part in writing and commenting on the manuscript.

AOB: Took part in overall analysis and interpretation of results and secured funding from Turkey side.

HIG: Did the homology modeling and structure analysis together with NSZ. Took part in writing the manuscript and commenting on the manuscript.

AK: Took part in purification, writing and commenting on the manuscript

MS: Took part in the construction and sequence analysis of the enzyme.

AK: Took part in cloning and production of the enzyme.

HA: Took part in sequence analysis and purification of the enzyme.

MB: Took part in planning and commenting on the manuscript

AAS: Took part in interpretation of results and commenting on the manuscript

SK: Took part in overall analysis and interpretation of results. Did the overall layout of manuscript, took part in writing and commenting on the manuscript and secured funding from Pakistan side.

All authors read and approved the manuscript.

Funding

This work was supported by Pakistan Science Foundation and TUBITAK Turkey [Project No. PSF-TUBITAK/Med/C-QAU (15).]

Declaration of Competing Interest

The authors report no declarations of interest.

Acknowledgements

The authors thank Pakistan Science Foundation and TUBITAK Turkey for providing financial assistance to carry out this work (Project No. PSF-TUBITAK/Med/C-QAU (15)).

The authors would also like to thank Higher Education commission Pakistan (HEC) for providing Indigenous Scholarship to Numan Saleh Zada.

Appendix A. Supplementary data

Supplementary material related to this article can be found, in the online version, at doi:https://doi.org/10.1016/j.enzmictec.2021.109799.

References

[1] M. Dashtban, H. Schraft, W. Qin, Fungal bioconversion of lignocellulosic residues; opportunities & perspectives, Int. J. Biol. Sci. 5 (2009) 578–595, https://doi.org/10.7150/ijbs.5.578.

[2] G. Banerjee, J.S. Scott-Craig, J.D. Walton, Improving enzymes for biomass conversion: a basic research perspective, Bioenergy Res. 3 (2010) 82–92, https://doi.org/10.1007/s12155-009-9067-5.

[3] M.V. Del Pozo, L. Fernández-Arrojo, J. Gil-Martínez, A. Montesinos, T. N. Chernikova, T.Y. Nechitaylo, A. Waliszek, M. Tortajada, A. Rojas, S.A. Huws, O. V. Golyshina, C.J. Newbold, J. Polaina, M. Ferrer, P.N. Golyshin, Microbial β-glucosidases from cow rumen metagenome enhance the saccharification of lignocellulose in combination with commercial cellulase cocktail, Biotechnol. Biofuels 5 (2012) 1–13, https://doi.org/10.1186/1754-6834-5-73.

[4] H. Teugjas, P. Väljamäe, Selecting β-glucosidases to support cellulases in cellulose saccharification, Biotechnol. Biofuels 6 (2013) 1–13, https://doi.org/10.1186/1754-6834-6-105.

[5] S. Brethauer, C.E. Wyman, Review: continuous hydrolysis and fermentation for cellulosic ethanol production, Bioresour. Technol. 101 (2010) 4862–4874, https://doi.org/10.1016/j.biortech.2009.11.009.

[6] Y. Zhao, B. Wu, B. Yan, P. Gao, Mechanism of cellobiose inhibition in cellulose hydrolysis by cellobiohydrolase, Sci. China Ser. C Life Sci. 47 (2004) 18–24, https://doi.org/10.1360/02yc0163.

[7] S. Wang, G. Liu, J. Wang, J. Yu, B. Huang, M. Xing, Enhancing cellulase production in Trichoderma reesei RUT C30 through combined manipulation of activating and repressing genes, J. Ind. Microbiol. Biotechnol. 40 (2013) 633–641, https://doi.org/10.1007/s10295-013-1253-y.

[8] G. Platas, R. Morón, I. González, J. Collado, O. Genilloud, F. Peláez, M.T. Diez, Production of antibacterial activities by members of the family Pseudonocardiaceae: influence of nutrients, World J. Microbiol. Biotechnol. 14 (1998) 521–527, https://doi.org/10.1023/A:1008874203344.

[9] S. Ariaeenejad, S. Nooshi-Nedamani, M. Rahban, K. Kavousi, A.G. Pirbalooti, S. Mirghaderi, M. Mohammadi, M. Mirzaei, G.H. Salekdeh, A novel high glucose-tolerant β-Glucosidase: targeted computational approach for metagenomic screening, Front. Bioeng. Biotechnol. 8 (2020) 813, https://doi.org/10.3389/fbioe.2020.00813.

[10] J. Sun, W. Wang, C. Yao, F. Dai, X. Zhu, J. Liu, J. Hao, Overexpression and characterization of a novel cold-adapted and salt-tolerant GH1 β-glucosidase from the marine bacterium Alteromonas sp. L82, J. Microbiol. 56 (2018) 656–664, https://doi.org/10.1007/s12275-018-8018-2.

[11] J. Wu, A. Geng, R. Xie, H. Wang, J. Sun, Characterization of cold adapted and ethanol tolerant β-glucosidase from Bacillus cellulosilyticus and its application for directed hydrolysis of cellobiose to ethanol, Int. J. Biol. Macromol. 109 (2018) 872–879, https://doi.org/10.1016/j.ijbiomac.2017.11.072.

[12] A. Wierzbicka-Woś, P. Bartasun, H. Cieśliński, J. Kur, Cloning and characterization of a novel cold-active glycoside hydrolase family 1 enzyme with β-glucosidase, β-fucosidase and β-galactosidase activities, BMC Biotechnol. 13 (2013) 22, https://doi.org/10.1186/1472-6750-13-22.

[13] X. Mao, Y. Hong, Z. Shao, Y. Zhao, Z. Liu, A novel cold-active and alkali-stable β-glucosidase gene isolated from the marine bacterium martelella mediterranea, Appl. Biochem. Biotechnol. 162 (2010) 2136–2148, https://doi.org/10.1007/s12010-010-8988-y.

[14] D.J. Park, Y.S. Lee, Y.L. Choi, Characterization of a cold-active β-Glucosidase from Paenibacillus xylanilyticus KJ-03 capable of hydrolyzing isoflavones Daidzin and genistin, Protein J. 32 (2013) 579–584, https://doi.org/10.1007/s10930-013-9520-3.

[15] A. Wierzbicka-Woś, P. Bartasun, H. Cieśliński, J. Kur, Cloning and characterization of a novel cold-active glycoside hydrolase family 1 enzyme with β-glucosidase, β-fucosidase and β-galactosidase activities, BMC Biotechnol. 13 (2013), https://doi.org/10.1186/1472-6750-13-22.

[16] T. Matsuzawa, M. Watanabe, K. Yaoi, Improved thermostability of a metagenomic glucose-tolerant β-glycosidase based on its X-ray crystal structure, Appl. Microbiol. Biotechnol. 101 (2017) 8353–8363, https://doi.org/10.1007/s00253-017-8525-9.

[17] W.Y. Jeng, N.C. Wang, M.H. Lin, C.T. Lin, Y.C. Liaw, W.J. Chang, C.I. Liu, P. H. Liang, A.H.J. Wang, Structural and functional analysis of three β-glucosidases from bacterium Clostridium cellulovorans, fungus Trichoderma reesei and termite Neotermes koshunensis, J. Struct. Biol. 173 (2011) 46–56, https://doi.org/10.1016/j.jsb.2010.07.008.

[18] S. Khan, T. Pozzo, M. Megyeri, S. Lindahl, A. Sundin, C. Turner, E.N. Karlsson, Aglycone specificity of Thermotoga neapolitana β-glucosidase 1A modified by mutagenesis, leading to increased catalytic efficiency in quercetin-3-glucoside hydrolysis, BMC Biochem. 12 (2011) 1–15, https://doi.org/10.1186/1471-2091-12-11.

[19] L. Zhao, J. Xie, X. Zhang, F. Cao, J. Pei, Overexpression and characterization of a glucose-tolerant β-glucosidase from Thermotoga thermarum DSM 5069T with high catalytic efficiency of ginsenoside Rb1 to Rd, J. Mol. Catal. B Enzym. 95 (2013) 62–69, https://doi.org/10.1016/j.molcatb.2013.05.027.

[20] J. Zhou, R. Zhang, P. Shi, H. Huang, K. Meng, T. Yuan, P. Yang, B. Yao, A novel low-temperature-active β-glucosidase from symbiotic Serratia sp. TN49 reveals four essential positions for substrate accommodation, Appl. Microbiol. Biotechnol. 92 (2011) 305–315, https://doi.org/10.1007/s00253-011-3323-2.

[21] K.S. Siddiqui, R. Cavicchioli, Cold-adapted enzymes, Annu. Rev. Biochem. 75 (2006) 403–433, https://doi.org/10.1146/annurev.biochem.75.103004.142723.

[22] S. Chen, Y. Hong, Z. Shao, Z. Liu, A cold-active β-glucosidase (Bgl1C) from a sea bacteria Exiguobacterium oxidotolerans A011, World J. Microbiol. Biotechnol. 26 (2010) 1427–1435, https://doi.org/10.1007/s11274-010-0317-7.

[23] Z. Fang, H. Peng, X. Zhang, Cloning and characterization of a beta-glucosidase from marine microbial metagenome with excellent glucose tolerance Post-translational modification View project, Artic. J. Microbiol. Biotechnol. 20 (2010) 1351–1358, https://doi.org/10.4014/jmb.1003.03011.

[24] D.J. Park, Y.S. Lee, Y.L. Choi, Characterization of a cold-active β-Glucosidase from Paenibacillus xylanilyticus KJ-03 capable of hydrolyzing isoflavones Daidzin and genistin, Protein J. 32 (2013) 579–584, https://doi.org/10.1007/s10930-013-9520-3.

[25] C.S. Chan, L.L. Sin, K.G. Chan, M.S. Shamsir, F.A. Manan, R.K. Sani, K.M. Goh, Characterization of a glucose-tolerant β-glucosidase from Anoxybacillus sp. DT3-1, Biotechnol. Biofuels 9 (2016) 174, https://doi.org/10.1186/s13068-016-0587-x.

[26] R. Goulding, Casarett & Doull's toxicology: the basic science of poisons, Postgrad. Med. J. 63 (1987) 1112 (Accessed February 27, 2021), https://www.ncbi.nlm.nih.gov/pmc/articles/PMC2428565/.

[27] K.J. Liew, L. Lim, H.Y. Woo, K.G. Chan, M.S. Shamsir, K.M. Goh, Purification and characterization of a novel GH1 beta-glucosidase from Jeotgalibacillus malaysiensis, Int. J. Biol. Macromol. 115 (2018) 1094–1102, https://doi.org/10.1016/j.ijbiomac.2018.04.156.

[28] M.E. Scharf, E.S. Kovaleva, S. Jadhao, J.H. Campbell, G.W. Buchman, D.G. Boucias, Functional and translational analyses of a beta-glucosidase gene (glycosyl hydrolase family 1) isolated from the gut of the lower termite Reticulitermes flavipes, Insect Biochem. Mol. Biol. 40 (2010) 611–620, https://doi.org/10.1016/j.ibmb.2010.06.002.

[29] J. Chang, I.H. Park, Y.S. Lee, S.C. Ahn, Y. Zhou, Y.L. Choi, Cloning, expression, and characterization of β-glucosidase from Exiguobacterium sp. DAU5 and transglycosylation activity, Biotechnol. Bioprocess Eng. 16 (2011) 97–106, https://doi.org/10.1007/s12257-010-0092-1.

[30] K. Wook, N. Soo Han, J. Hwan Kim, Purification and Characterization of Beta-Glucosidase from Weissella cibaria 37, J. Microbiol. Biotechnol. 22 (2012) 1017–7825, https://doi.org/10.4014/jmb.1206.06007.

[31] Y. Yuan, F. Xu, J. Yao, Y. Hu, J. Wang, T. Zhao, Y. Zhou, J. Gao, Cloning, expression and biochemical characterization of a GH1 β-glucosidase from Cellulosimicrobium cellulans, Biocatal. Biotransformation 36 (2018) 362–371, https://doi.org/10.1080/10242422.2017.1395415.

[32] J. Pei, Q. Pang, L. Zhao, S. Fan, H. Shi, Thermoanaerobacterium thermosaccharolyticum β-glucosidase: a glucose-tolerant enzyme with high specific activity for cellobiose, Biotechnol. Biofuels 5 (2012) 1–10, https://doi.org/10.1186/1754-6834-5-31.

[33] S.K. Mishra, N.S. Sangwan, R.S. Sangwan, Purification and physicokinetic characterization of a gluconolactone inhibition-insensitive β-glucosidase from andrographis paniculata nees, Leaf, Prep. Biochem. Biotechnol. 43 (2013) 481–499, https://doi.org/10.1080/10826068.2012.759966.

[34] J. Boyle, in: 4th ed., in: D. Nelson, M. Cox (Eds.), Lehninger Principles of Biochemistry, 33, Biochem. Mol. Biol. Educ., 2005, pp. 74–75, https://doi.org/10.1002/bmb.2005.494033010419.
[35] H.M. Pyeon, Y.S. Lee, Y.L. Choi, Cloning, purification, and characterization of GH3 β-glucosidase, MtBgl85, from Microbulbifer thermotolerans DAU221, PeerJ 2019 (2019) e7106, https://doi.org/10.7717/peerj.7106.
[36] F.F. Zanoelo, M. de L.T. de M. Polizeli, H.F. Terenzi, J.A. Jorge, β-Glucosidase activity from the thermophilic fungus Scytalidium thermophilum is stimulated by glucose and xylose, FEMS Microbiol. Lett. 240 (2004) 137–143, https://doi.org/10.1016/j.femsle.2004.09.021.
[37] J.A. Pérez-Pons, X. Rebordosa, E. Querol, Properties of a novel glucose-enhanced β-glucosidase purified from Streptomyces sp. (ATCC 11238), Biochim. Biophys. Acta (BBA)/Protein Struct. Mol. 1251 (1995) 145–153, https://doi.org/10.1016/0167-4838(95)00074-5.
[38] D. Mariano, Characterization of glucose-tolerant β-glucosidases used in biofuel production under the bioinformatics perspective: a systematic review OCELUS-automatizing the linear welding process using computer vision view project, Researchgate.Net. (2017), https://doi.org/10.4238/gmr16039740.
[39] B.C. Saha, R.J. Bothast, Production, purification, and characterization of a highly glucose-tolerant novel beta-glucosidase from Candida peltata, Appl. Environ. Microbiol. 62 (1996).
[40] C. Riou, J.M. Salmon, M.J. Vallier, Z. Günata, P. Barre, Purification, characterization, and substrate specificity of a novel highly glucose-tolerant β-glucosidase from Aspergillus oryzae, Appl. Environ. Microbiol. 64 (1998) 3607–3614, https://doi.org/10.1128/aem.64.10.3607-3614.1998.
[41] A. Belancic, Z. Gunata, M.J. Vallier, E. Agosin, β-glucosidase from the grape native yeast Debaryomyces vanrijiae: purification, characterization, and its effect on monoterpene content of a muscat grape juice, J. Agric. Food Chem. 51 (2003) 1453–1459, https://doi.org/10.1021/jf025777l.
[42] G. Gao, A. Wang, B.L. Gong, Q.Q. Li, Y.H. Liu, Z.M. He, G. Li, A novel metagenome-derived gene cluster from termite hindgut: encoding phosphotransferase system components and high glucose tolerant glucosidase, Enzyme Microb. Technol. 84 (2016) 24–31, https://doi.org/10.1016/j.enzmictec.2015.12.005.
[43] D.C.B. Mariano, C. Leite, L.H.S. Santos, L.F. Marins, K.S. Machado, A.V. Werhli, L. H.F. Lima, R.C. de Melo-Minardi, Characterization of glucose-tolerant β-glucosidases used in biofuel production under the bioinformatics perspective: a systematic review, Genet. Mol. Res. 16 (2014), https://doi.org/10.4238/gmr16039740.
[44] Y. Yang, X. Zhang, Q. Yin, W. Fang, Z. Fang, X. Wang, X. Zhang, Y. Xiao, A mechanism of glucose tolerance and stimulation of GH1 β-glucosidases, Sci. Rep. 5 (2015) 1–12, https://doi.org/10.1038/srep17296.
[45] P.O. De Giuseppe, T.D.A.C.B. Souza, F.H.M. Souza, L.M. Zanphorlin, C.B. Machado, R.J. Ward, J.A. Jorge, R.D.P.M. Furriel, M.T. Murakami, Structural basis for glucose tolerance in GH1 β-glucosidases, Acta Crystallogr. Sect. D Biol. Crystallogr. 70 (2014) 1631–1639, https://doi.org/10.1107/S1399004714006920.